Advances in Cement Research
Volume 26 Issue 1

Impact of environmental moisture on C_3A polymorphs in the absence and presence of $CaSO_4 \cdot 0{\cdot}5\ H_2O$
Dubina, Plank, Black and Wadsö

Advances in Cement Research, 2014, **26**(1), 29–40
http://dx.doi.org/10.1680/adcr.12.00062
Paper 1200062
Received 16/10/2012; revised 16/04/2013; accepted 06/07/013
Published online ahead of print 27/09/2013

ice
Institution of Civil Engineers
publishing

Impact of environmental moisture on C_3A polymorphs in the absence and presence of $CaSO_4 \cdot 0{\cdot}5\ H_2O$

Elina Dubina
PhD student, Technische Universität München, Lehrstuhl für Bauchemie, Munich, Germany

Johann Plank
Professor and Chair for Construction Chemistry, Technische Universität München, Lehrstuhl für Bauchemie, Munich, Germany

Leon Black
Senior Lecturer in Civil Engineering Materials, Institute for Resilient Infrastructure, School of Civil Engineering, University of Leeds, Leeds, UK

Lars Wadsö
Professor, Department of Building Materials, University of Lund, Lund, Sweden

The phenomenon of water vapour sorption by anhydrous C_3A polymorphs both in the absence and in the presence of $CaSO_4 \cdot 0{\cdot}5\ H_2O$ was studied utilising dynamic and static sorption methods. It was found that orthorhombic C_3A starts to sorb water at 55% relative humidity (RH) and cubic C_3A at 80% RH. Also, C_3A_o sorbs a higher amount of water which is predominantly physically bound, whereas C_3A_c preferentially interacts with water by chemical reaction. In the presence of calcium sulfate hemihydrate, ettringite was observed as the predominant pre-hydration product for both C_3A modifications: that is, ion transport had occurred between C_3A and sulfate. Environmental scanning electron microscopic imaging revealed that in a moist atmosphere, a liquid water film condenses on the surface of the phases as a consequence of capillary condensation between the particles. C_3A and sulfate can then dissolve and react with each other. Seemingly, pre-hydration is mainly facilitated through capillary condensation and less through surface interaction with gaseous water molecules.

Notation

d_{50}	calcium aluminate hydrate phases average particle size
M_t	amount of water sorbed by the sample at time t
p	water (H_2O) under actual test conditions
p_0	partial water pressure at saturation
R	universal gas constant
r	radius of the pores or initial spaces
t	time
W_0	weight of the sample at the beginning of the experiment
W_t	weight of the sample at sorption time t
σ	surface tension of water
ρ	density of the sample

Introduction

Ordinary Portland cement (OPC) is a moisture-sensitive material and may take up water vapour during the manufacturing process or later on by inappropriate conditions occurring during its transport or storage (Hansen and Clausen, 1974; Richartz, 1973; Sprung, 1978). The phenomenon of water vapour sorption by cement powder exposed to humidity is known as pre-hydration of cement (Breval, 1977; Jensen *et al.*, 1999). Pre-hydration of cement may lead to failures that are more prevalent in climates characterised by high temperatures and humidities. In previous works, several consequences of pre-hydration for the chemical and engineering properties of cement have been reported. These include: increased setting time, decreased compressive strength and heat of hydration, altered rheological properties and poor response to superplasticiser addition (Deng *et al.*, 2002; Maltese *et al.*, 2007; Schmidt *et al.*, 2007; Sylla, 1975; Theisen and Johansen, 1975; Whittaker *et al.*, 2013; Winnefeld, 2008).

In order to secure control of cement performance in the field and thus also of concrete performance, it is important to understand the mechanisms behind the interactions of cement with water vapour. Owing to the complex nature of cement, it is challenging to identify the key processes occurring during sorption of water on the surfaces of cement particles. Previous studies have shown that the individual clinker minerals C_3S, C_2S, C_3A and C_4AF have fundamentally different sensitivities to moisture (Dubina *et al.*, 2010; Jensen, 1995).

The current authors have investigated the physicochemical effects of water sorption on the surfaces of pure individual clinker phases, plus those of different sulfates and free lime (Dubina *et al.*, 2011). The authors determined the relative humidity (RH) thresholds at which early-stage hydration (up to 11 h) of these cement constituents in moist atmospheres started to occur, and the amount of water sorbed per unit of surface area. The

experiments demonstrated that among all cement components, orthorhombic C_3A and free lime were the ones which started to sorb water at particular low RH values ($< 55\%$). Additionally, they sorbed the highest amounts of water. Cubic C_3A and C_4AF followed next, while C_3S and C_2S, the main clinker constituents, were the least reactive phases.

However, the study of pre-hydration of individual cement constituents does not account for interactions between different phases, which can take place during pre-hydration of actual cements. For example, it is well established that at the early stage of its hydration with liquid water, C_3A can react with sulfates to form AF_m or AF_t phases (Black *et al.*, 2006; Brown *et al.*, 1984; Minard *et al.*, 2007; Pourchet *et al.*, 2009). Thus, formation of those phases may significantly affect further sorption of water vapour by cement. Furthermore, Kirchheim *et al.* (2009) showed that there are important differences between the hydration of the two C_3A polymorphs (cubic and orthorhombic) with gypsum. Therefore, it is of interest to have a better understanding of the interaction of each C_3A polymorph with calcium sulfates when exposed to different relative humidities.

In an earlier study it was reported that cubic C_3A reacted with gypsum when it was pre-hydrated (Breval, 1979). Yet there are no studies which compare the behaviour of the two C_3A polymorphs (cubic and orthorhombic) when exposed to moisture in the presence of calcium sulfate hemihydrate, and the mechanism underlying this pre-hydration reaction. More specifically, it is unknown whether pre-hydration is solely a reaction between C_3A with sulfates and gaseous water vapour, or whether it occurs as a consequence of water vapour condensation, which then allows C_3A and sulfate to react in solution.

In this study, specific water sorption experiments were performed to gain an understanding of the principal interactions occurring during pre-hydration between the C_3A polymorphs in the absence and presence of calcium sulfate hemihydrate (subsequently abbreviated as 'hemihydrate', and chosen for its higher solubility and dissolution rate compared to gypsum or anhydrite). From this, the behaviours of the two C_3A polymorphs were compared.

Materials and methods

Materials

Pure, undoped cubic C_3A and orthorhombic C_3A doped with 4 wt% Na_2O were synthesised from calcium carbonate and aluminium oxide according to Dubina *et al.* (2011). In the preparation of C_3A_o, sodium nitrate was used as a source for Na_2O. The sintered samples were removed from the oven, allowed to cool in air for 3 min and then immediately placed in the cup of a ball mill (Planetary Mono Mill Pulverisette 6 classic line, Fritsch, Idar-Oberstein, Germany). Grinding was performed for 10 min at 250 r/min at a temperature of 21°C and a RH of 20%. No grinding agent was added in the milling process.

Precautions were taken to prevent reaction with atmospheric carbon dioxide and water vapour by storing the freshly ground samples in sealed 20 ml glass bottles placed in a vacuum desiccator containing silica gel as a drying agent.

According to quantitative X-ray diffraction (XRD) analysis using Rietveld refinement, the C_3A phases were $99 \pm 0{\cdot}5$ wt% pure. The XRD patterns of the cubic and orthorhombic C_3A samples are presented in Figure 1. Their average particle size (d_{50} value) and specific surface area (Brunauer–Emmett–Teller (BET), N_2) are given in Table 1.

The sample of β-modification of calcium sulfate hemihydrate (purity 97 wt%) was obtained from Sigma-Aldrich (Taufkirchen, Germany). The average particle size and specific surface area were 10·4 μm and 12 000 cm^2/g, respectively (Table 1). Binary mixtures of individual cubic and orthorhombic C_3A respectively with hemihydrate were prepared by manually blending the C_3A and hemihydrate powders at a molar ratio of 1:1.

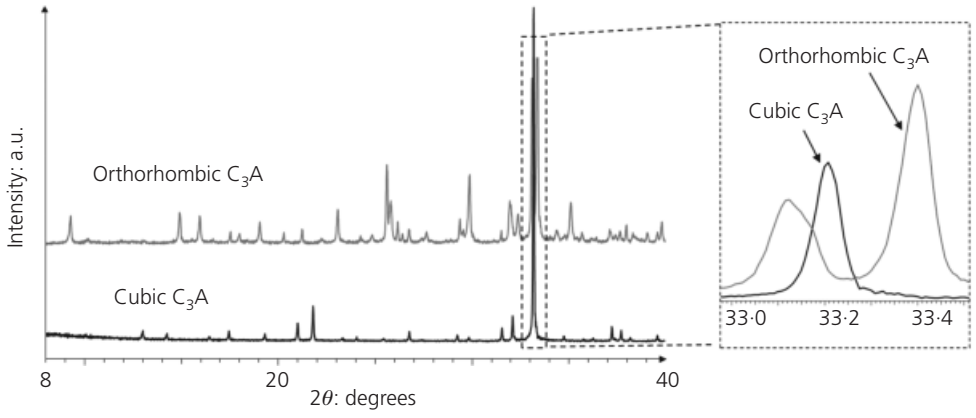

Figure 1. X-ray diffraction patterns of cubic and orthorhombic C_3A phases as prepared, shown in the range of 8–40 (2θ degrees scale)

Phase	Average particle size (d_{50} value): μm	Specific surface area (BET): cm^2/g
Cubic C_3A	6·2	7800
Orthorhombic C_3A	10·0	7000
$CaSO_4 \cdot 0{\cdot}5\ H_2O$	10·4	12 000

Table 1. Average particle size (d_{50} value) and specific surface area (BET) of the cubic and orthorhombic C_3A modifications prepared for this study

Methods

Exposure of samples to water vapour

For the determination of the water vapour sorption behaviour of the various samples, both dynamic and semi-equilibrium (static) water sorption methods were used. In both experiments, the temperature was held constant at 20°C.

A sorption balance (DVS Advantage, Surface Measurement Systems Ltd, London, UK) was used to measure the moisture uptake using the dynamic method. Further details on this instrument and the general set-up can be found in Dubina *et al.* (2011). For analysis, 0·015–0·05 g of a binary mixture (C_3A + hemihydrate) were placed in a sample pan, which was then transferred into a climate chamber where the desired RH was obtained by mixing a proportional amount of dry and humid nitrogen gas. Two different exposure protocols were used during the dynamic vapour sorption tests, as described below.

In the first regime, RH was continuously increased from 1% to 95% RH at a constant rate of approximately 0·16% RH per minute, as described in Dubina *et al.* (2011). This ramp regime provided a mass change profile and made it possible to assess the threshold value of RH (onset point) at which a sample started to sorb water. In the second regime, RH was increased from 1% to 95% RH in 10% RH steps to the desired RH and then kept at this level, as shown in Figure 2. The duration of exposure at each RH was set at either 1 h for short-duration experiments and at 5 h for long-duration experiments. At the beginning and end of each experiment, RH was set to 1% RH.

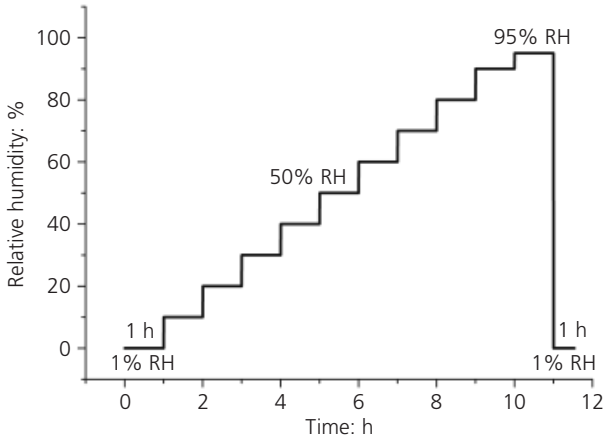

Figure 2. Test protocol for the dynamic water vapour sorption experiment whereby relative humidity is increased in 1 h steps over time

In this study, physically bound water is defined as water which can be removed by drying at 1% RH for 1 h only, while non-removable water was considered to be bound chemically (irreversibly sorbed).

For the semi-equilibrium (static) regime the relative humidity environment was realised by keeping the samples (0·15–0·50 g) in a desiccator above saturated salt solutions. Exposure period was 21 d. The salts used and their relative humidity values are given in Table 2.

For the experiments in the presence of calcium sulfate hemihydrate, the binary mixtures were weighed accurately (this value was designated as W_0), and then stored for 21 d at a constant temperature of 20°C ± 1°C under different relative humidities. The weight increase of the samples at sorption time t was measured by quickly weighing them on a digital balance. This

Salt	K-acetate	$MgCl_2$	K_2CO_3	NaBr	NaCl	KCl	KNO_3
Concentration: g/l[a]	2700	700	1350	1200	500	500	500
RH: %	23	33	43	60	75	85	95
$p(H_2O)$: kPa	0·54	0·77	1·01	1·40	1·76	1·99	2·22

[a] With solid salt at the bottom of the salt solution.

Table 2. The saturated salt solutions used in the experiments, the corresponding relative humidity values at 20°C obtained from them and the values for partial water pressure calculated from the saturation vapour pressure of water (2·34 kPa) at RH = 100% (Greenspan, 1977)

value was noted as W_t. The weight increases were monitored over a period of 21 d. The percentage mass of water sorbed by a binary mixture at time t was calculated as

$$M_t = \frac{W_t - W_0}{W_0} \times 100\% \quad (1)$$

Instrumentation

Samples were analysed by quantitative XRD using a Bruker D8 Advance X-ray diffractometer (Bruker AXS, Karlsruhe, Germany) with Bragg – Brentano geometry, equipped with a two-dimensional detector (Vantec – 1, Bruker AXS, Karlsruhe, Germany) operated at an accelerating voltage of 40 keV on a CuK_α anode, irradiation intensity of 30 mA, and 40 scans in steps of 0·02°/s. Cement hydrates were identified by comparison with Diffract Plus EVA Application V.8·0 and JCPDS PDF-2 database (JCPDS, 2003).

The average particle size (d_{50} value) of all phases tested was measured by laser granulometry (Cilas 1064, Cilas, Marcoussis, France) using isopropyl alcohol as a base fluid and ultrasound to disagglomerate the particles before the measurement.

The specific surface area of all samples was determined by nitrogen adsorption (BET method) employing a Nova 4000e surface area analyser from Quantachrome (Odelzhausen, Germany).

Environmental scanning electron microscopic (ESEM) and scanning electron microscopic (SEM) images were obtained on a FEI XL 30 FEG instrument (FEI, Eindhoven, Netherlands) equipped with a Peltier cooling stage and a gaseous secondary electron detector. One set of samples was investigated under low vacuum conditions (1 mbar H_2O pressure, corresponding to ~ 4% RH at room temperature). Samples were not coated and were examined before and after their exposure to RH in a sorption balance or in a desiccator over various periods of time.

For selected samples, in situ observations of the development of pre-hydration products were performed using the ESEM mode. For this, anhydrous samples were placed on the cooling stage in the microscope chamber whereupon the temperature was lowered to 3°C and the water vapour pressure was raised to ~ 6·3 mbar (corresponding to 85% RH) for 1·5 h. To allow high-resolution imaging, the pressure was lowered to ~ 1·7 mbar (corresponding to ~ 7% RH) during imaging.

Results and discussion

Water sorption behaviour of individual C_3A polymorphs

Total water sorption

Applying the ramp regime, cubic and orthorhombic C_3A showed significantly different behaviours (Figure 3). Orthorhombic C_3A started to sorb water already at ~ 55% RH, which is far below the onset point of 80% RH observed for cubic C_3A. This indicates that orthorhombic C_3A is more susceptible to moisture than cubic C_3A.

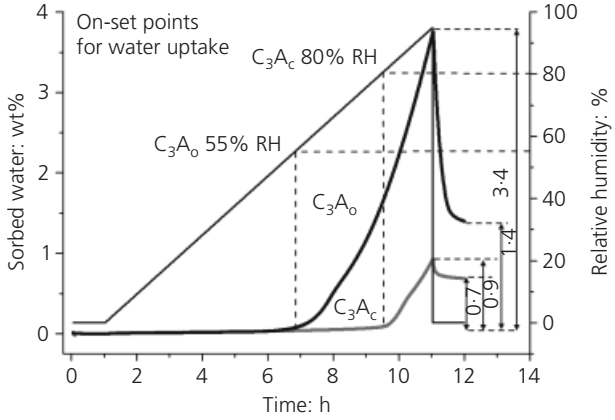

Figure 3. Water vapour sorption isotherms of cubic and orthorhombic C_3A, determined on a sorption balance at 20°C using ramp mode and measured over a period of 11 h

Under these conditions, when RH reached 95%, cubic C_3A had sorbed ~ 0·9 wt% of water, based on its dry mass. Thereafter, when RH was lowered to 1%, 0·7 wt% could not be removed and thus were considered as bound by chemical reaction. In comparison, orthorhombic C_3A had sorbed a total of ~ 3·4 wt% of water, with ~ 1·4 wt% bound chemically. The water sorption behaviour of the two C_3A polymorphs is in line with their relative reactivities in cement hydration. There, it is well established that orthorhombic C_3A (which contains a higher amount of Na_2O dope) is more reactive with sulfate than the cubic C_3A polymorph, which is low in Na_2O content.

Following the water vapour sorption experiment, all samples were analysed by XRD and SEM. XRD revealed no discernible differences between pre-hydrated and fresh samples, with the amount of surface hydrates formed being insignificant compared to the non-reacted bulk material.

However, SEM analysis revealed significant differences in the surface appearance of the two polymorphs (Figure 4). Undoped C_3A_c showed considerably fewer pre-hydration products than C_3A_o. For cubic C_3A, preferential nucleation of C-A-H phases between grains or on grain edges was observed. For the sodium-doped C_3A_o, after water vapour exposure the initially smooth surface was almost completely covered by very fine crystals of Na_2CO_3, as indicated by elemental energy-dispersive X-ray (EDX) mapping. Additionally, C-A-H phases were found on the surface.

The presence of alkalis has a major impact on the water vapour sorption behaviour of C_3A. Orthorhombic C_3A shows a tendency

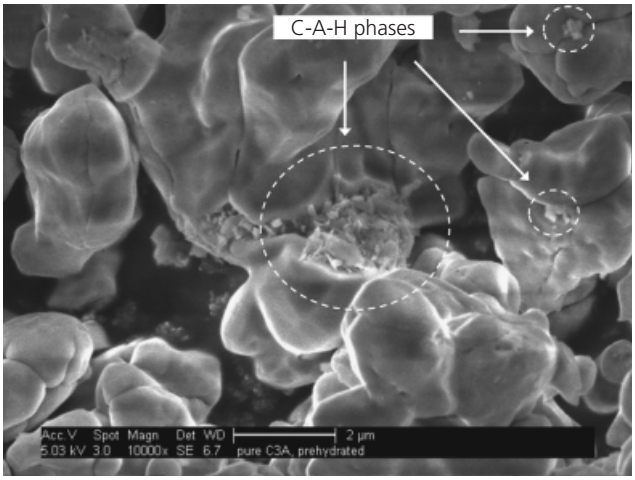

(a)

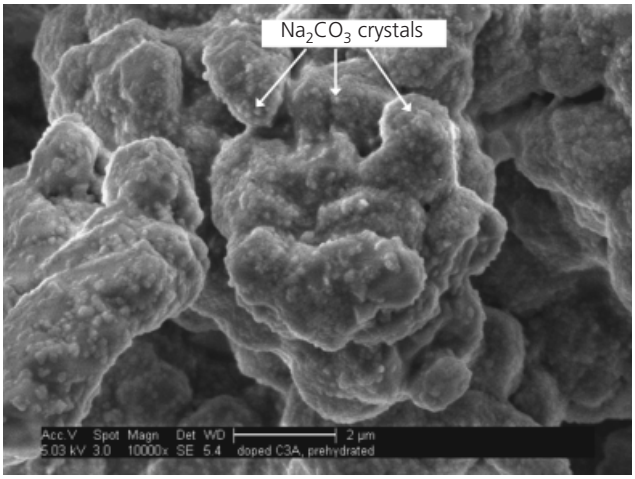

(b)

Figure 4. SEM images of the C_3A polymorphs pre-hydrated for 10 h using ramp regime and subsequent drying at 1% RH for 1 hr at 20°C: (a) pure, cubic C_3A; (b) doped, orthorhombic C_3A

to selectively exclude sodium ions from its crystal structure (Glasser and Marinho, 1984). This process can change both the surface characteristics and also the bulk properties of C_3A. When orthorhombic C_3A comes in contact with water vapour, then it reacts to form C-A-H phases and sodium ions are released as NaOH which will then quickly undergo carbonation.

Most interesting and important, however, was evidence of condensed water films, occurring mainly in the interstitial spaces and sometimes on the surfaces of the C_3A particles exposed to moisture. Figure 5 shows as example an in situ ESEM image of C_3A_c exposed for 30 min to 85% RH in the microscope chamber. The micrograph reveals a thin water film which bridged two adjacent C_3A particles. Such films were also observed when studying C_3A_o samples.

Obviously, interaction of these phases with humidity is not

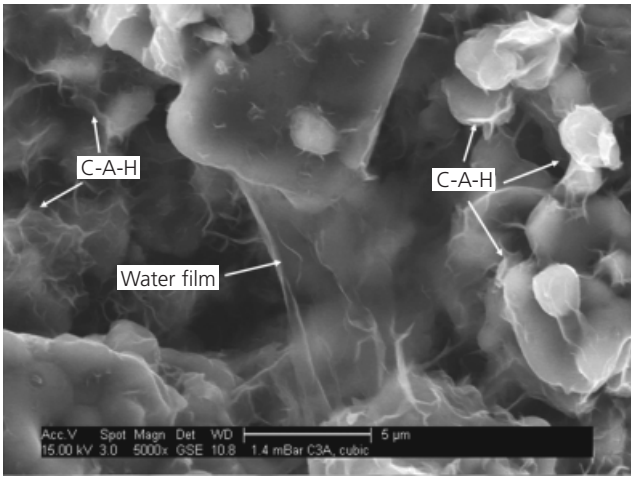

Figure 5. ESEM image of cubic C_3A, pre-hydrated for 30 min in the ESEM chamber at 4·5°C and 85% RH, exhibiting a film of condensed liquid water between the particles

limited to physicochemical reactions whereby gaseous water molecules first sorb onto the surfaces of the mineral phases and then produce initial hydration products from each individual phase. In the present study, a different mode of interaction was observed involving liquid condensed water, whereby the phases first dissolve, then hydrates resulting even from dissolved ions of two different mineral species are precipitated from an oversaturated solution. This mechanism is based on capillary condensation of water in the interstitial spaces between the clinker particles which can be described by Kelvin's equation

$$\ln\left(\frac{p}{p_0}\right) = -\frac{\sigma}{RT\rho r} \quad (2)$$

where p is partial pressure of water under actual test conditions, p_0 is partial water pressure at saturation, σ is surface tension of water, R is a universal gas constant, ρ is density of the sample and r is radius of the pores or initial spaces.

According to Equation 2 it is obvious that the smaller the pore size, the lower the RH at which capillary condensation occurs. In this study, a broad distribution of pore sizes ranging from 50 nm to 1 μm was evident between the C_3A particles (Figures 4 and 5). Electron micrographs showed evidence of water films on all samples after only a few minutes of exposure to moist air, and the first hydration products become visible immediately after the films appeared. The amount of hydrates became more abundant with exposure time.

The observation that pre-hydration – at least partially – occurs by way of a liquid film of condensed water is of great significance. It suggests that during the process of pre-hydration, cement constituents can interact with each other in a similar

manner as during normal hydration after mixing cement with water. This concept was probed further when the binary mixtures of C_3A and hemihydrate were tested later. However, it must be considered that the chemical potential of water is decreasing by reducing the water vapour pressure (RH) or by presence of alkali ions (e.g. sodium in orthorhombic C_3A) with high ionic strengths leading to precipitation of hydrates with lower water content than at high water activities, for example during hydration with liquid water (Baquerizo *et al.*, 2012).

Impact of exposure time on water sorption

The water vapour sorption process is dependent on different factors, such as temperature, exposure time, RH and specific properties of the material under investigation. As a system may take time to reach equilibrium, the amount of sorbed water may vary with respect to time when the sample is exposed to humidity. To study the impact of storage time on the amounts of chemically and physically bound water, cubic and orthorhombic C_3A samples were exposed to humidity using the step mode.

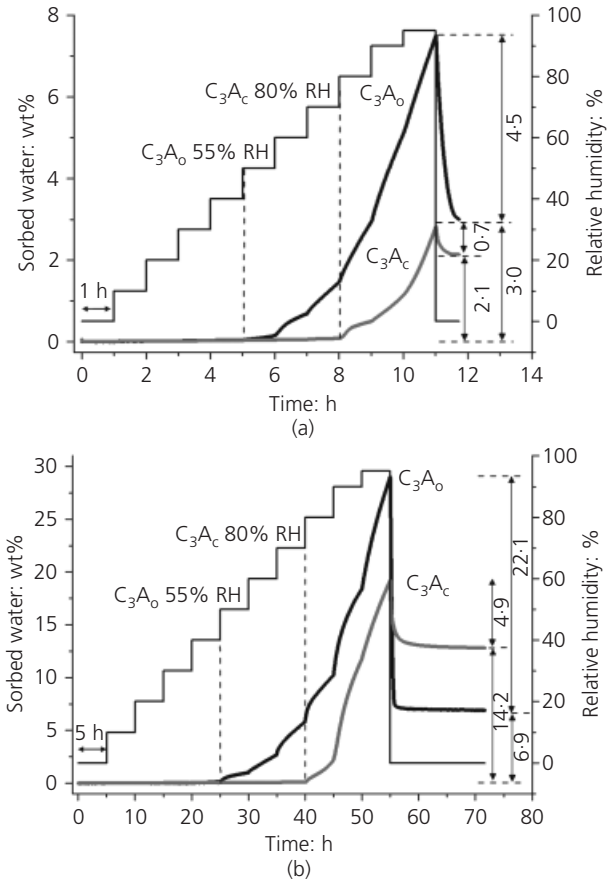

Figure 6. Water vapour sorption isotherms of cubic and orthorhombic C_3A, determined on a sorption balance at 20°C using the RH step mode and measured over a total time period of (a) 11 h and (b) 55 h

Figure 6 shows the time-dependent evolution of mass change for both samples at increased RH. The exposure time for each RH step was increased from 1 h (short exposure) to 5 h (long exposure), and the amounts of physically and chemically bound water were calculated based on the initial dried mass of samples.

The extended exposure times had no influence on the thresholds for water uptake. Orthorhombic and cubic C_3A samples started to take up noticeable amounts of water vapour at RH values of 50% RH and 80% RH respectively (Figure 6). These RH values are in good agreement with the onset points found before using the ramp regime (55% RH for orthorhombic C_3A and 80% RH for cubic C_3A; see Figure 3). However, the duration of the experiments did affect the total amounts of water sorbed by each sample. When exposed to 5 h steps, cubic C_3A sorbed almost 7 times more water than when exposed to 1 h steps, whereas orthorhombic C_3A sorbed 4 times more water. Despite this, for cubic C_3A the ratio between chemically and physically bound water was independent of the duration of the experiment, remaining at ~3 for both short (2·1/0·7 wt%) and long (14·2/4·9 wt%) exposure. For orthorhombic C_3A, however, the ratio changed significantly. When humidity was increased in 1 h steps, the ratio of chemically to physically bound water was 0·7. It decreased to 0·3 for the experiments applying 5 h steps. This indicates that under prolonged exposure to humidity, orthorhombic C_3A undergoes fewer chemical reactions and preferentially sorbs water physically. Consequently, independent of exposure times, cubic C_3A generally predominantly interacts with water vapour through chemical reactions while orthorhombic C_3A preferentially sorbs water physically.

Another significant difference was observed in the total amounts of water bound chemically on each sample after drying at 1% RH. Here, after longer exposure times, cubic C_3A bound more water chemically than orthorhombic C_3A (14·2 wt% against 6·9 wt%). Characterisation of the samples by XRD after exposure to humidity showed no apparent changes after short exposure (11 h). However, for orthorhombic C_3A reflections for katoite (C_3AH_6) were observed after long exposure (Figure 7). No additional reflections from sodium containing phases (e.g. Na_2CO_3) were found for the orthorhombic phase.

It should be noted that under real conditions, when a C_3A or cement sample is exposed to humid air, no subsequent drying will occur at the end of the exposure period. Thus, the total amount of water sorbed there will also include physically bound water. Additionally, throughout this experiment carbon dioxide was rigorously excluded to minimise the formation of various carbonate species. Such a condition differs significantly from actual storage environments.

Influence of particle size on water sorption

Another factor which may greatly influence the total amount of water sorbed is the particle size and therefore the specific surface area of a sample and the pore sizes for capillary condensation. To determine the impact of particle size on the water vapour sorption

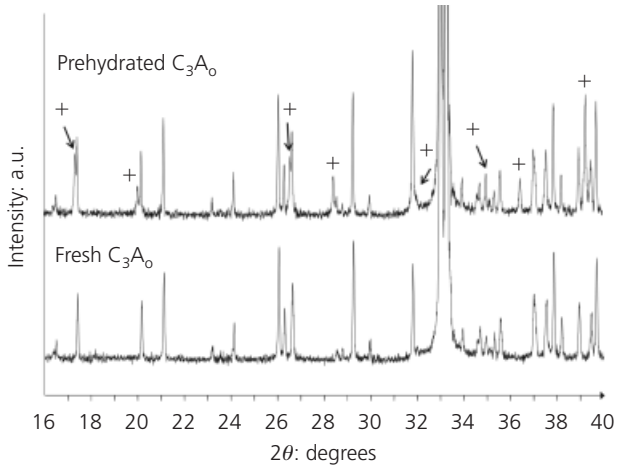

Figure 7. X-ray diffraction patterns recorded before and after exposure of orthorhombic C_3A to RH over a period of 55 h using the ramp regime: + – katoite (JCPDS no. 24–0217), unlabelled reflections belong to orthorhombic C_3A

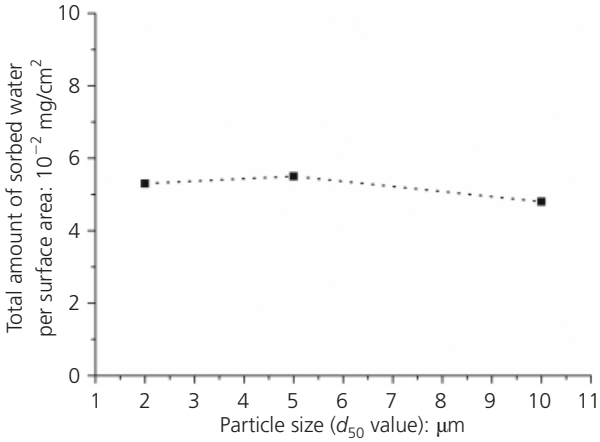

Figure 9. Plot of total amount of sorbed water per surface area (after exposure of sample to RH at 20°C for 55 h using the step mode) as a function of particle size (d_{50} value) of C_3A_o

behaviour, orthorhombic C_3A with an initial average particle size (d_{50} value) of 10 μm was ground to 5 μm and 2 μm respectively. Figure 8 shows the isotherms obtained for the three samples over 55 h of exposure. As expected, smaller samples, which possess higher specific surface areas, sorbed greater amounts of water. For example, the C_3A powder ground to 2 μm sorbed ~ 57% of its own mass, against 30% for the 10 μm sample. To determine the impact of surface area, the values of sorbed mass of water per unit mass of phase were converted into values per unit of surface area, and the results shown in Figure 9. The amount of water sorbed per unit surface is independent of particle size and lies at ~0·05 mg/cm^2. Similarly, the onset of water uptake was independent of particle size. It started when RH reached 50%, in good agreement with the results presented earlier (see Figure 3).

Binary mixtures

Dynamic water vapour sorption

To study the behaviour of water sorption in the presence of sulfates, the cubic and orthorhombic C_3A polymorphs were exposed to a ramped RH regime in the presence of hemihydrate.

Figure 10 shows the cumulative amount of water sorbed by the binary mixtures. Below 64% RH, the sorption profiles of both C_3A polymorphs exhibit almost identical characteristics. Furthermore, both modifications show step-like mass increase over the range 34–60% RH, which can be attributed to the hemihydrate. This step also occurred in the mass profile of pure hemihydrate exposed to humidity (Dubina *et al.*, 2011), where pure hemihydrate showed two onset points, one at ~34% RH and one at ~78% RH, with an inflection point at ~44% RH.

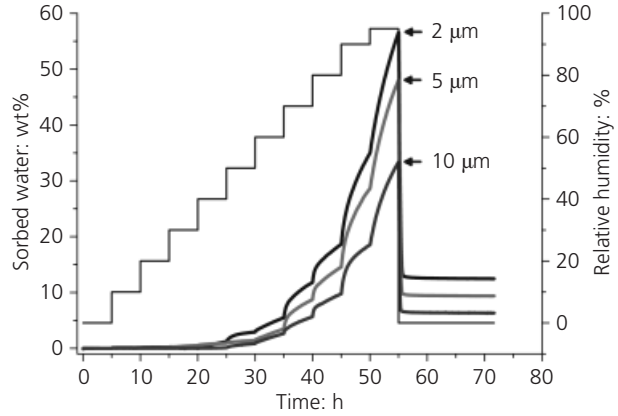

Figure 8. Water vapour sorption isotherms for orthorhombic C_3A ground to average particle sizes of 10 μm, 5 μm and 2 μm respectively, determined on a sorption balance at 20°C over a period of 55 h using step mode

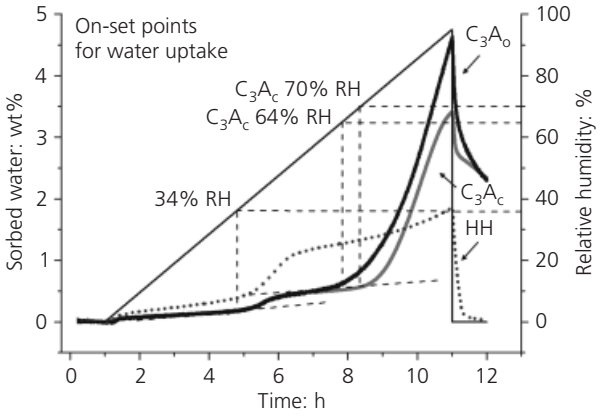

Figure 10. Water vapour sorption isotherms for pure $CaSO_4 \cdot 0{\cdot}5\ H_2O$ and for cubic and orthorhombic C_3A dry-blended with hemihydrate, determined on a sorption balance at 20°C over a period of 11 h using the ramp regime

The shapes of the water sorption profiles of the binary mixtures imply that at lower RHs, no chemical reaction occurs between C_3A and hemihydrate during pre-hydration; the mixtures sorb minimal amounts of moisture on their surfaces, possibly by hydrogen bonding. Additionally, for the binary mixture containing orthorhombic C_3A, the onset point occurred at a slightly lower RH (64%) than for the binary mixture containing cubic C_3A (70% RH). This suggests that the sodium ions present in orthorhombic C_3A lower the onset point.

Table 3 gives a comparison of the total amounts of water sorbed by cubic and orthorhombic C_3A at 20°C in the absence and presence of hemihydrate using the ramp regime. The table presents the amount of water sorbed by mass percentage and per unit of surface area (BET) of C_3A. The values show that when hemihydrate was present, both C_3A polymorphs sorbed higher amounts of water than in the absence of sulfate, with the effect on cubic C_3A being much more pronounced than for C_3A_o. XRD analysis performed for the binary mixtures after exposure to moisture showed formation of ettringite for both modifications, confirming that C_3A reacts chemically with hemihydrate (Figure 11).

C_3A polymorph	Mass change after exposure to humidity			
	Hemihydrate absent		Hemihydrate present	
	wt%	10^{-7}g/cm^2	wt%	10^{-7}g/cm^2
Cubic	0·92	11·8	3·42	38·9
Orthorhombic	3·60	51·4	4·60	54·8

Table 3. Comparison of the total amounts of water sorbed by cubic and orthorhombic C_3A at 20°C in the absence and presence of hemihydrate over 11 h using the ramp programme

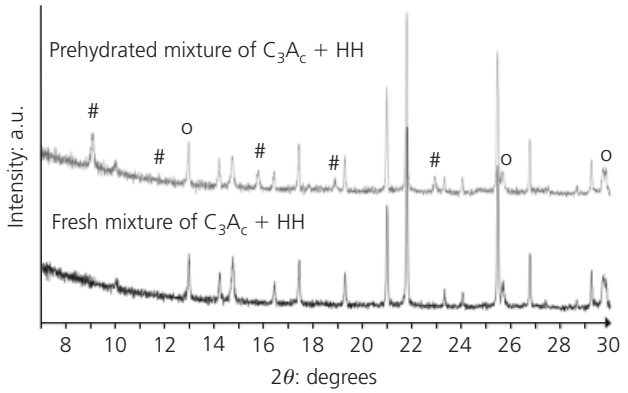

Figure 11. X-ray diffraction patterns of a binary mixture of cubic C_3A with hemihydrate recorded before and after exposure to RH over a period of 11 h using a ramp regime: # – ettringite (JCPDS no. 42–1451), o – hemihydrate (JCPDS no. 41–0224), unlabelled reflections belong to cubic C_3A

In order to determine whether the pre-hydration reaction observed between C_3A and hemihydrate occurs with water vapour (gas molecules) or by way of condensation of water vapour followed by liquid-phase reactions, in situ ESEM monitoring of the pre-hydration of C_3A with hemihydrate was performed. For this purpose, the binary mixtures were exposed to 85% RH at 4·5°C for 1·5 h in the chamber of an ESEM instrument. Figure 12(a) clearly shows evidence of a liquid water film immediately at the beginning of the imaging. Later on, formation of nano-sized ettringite needles on the surface of C_3A (here: orthorhombic polymorph) was evidenced, as shown in Figure 12(b). This result is most interesting because ettringite formation is possible only if ions are dissolved from both C_3A and hemihydrate and then react in the liquid phase into ettringite. Thus, this experiment shows

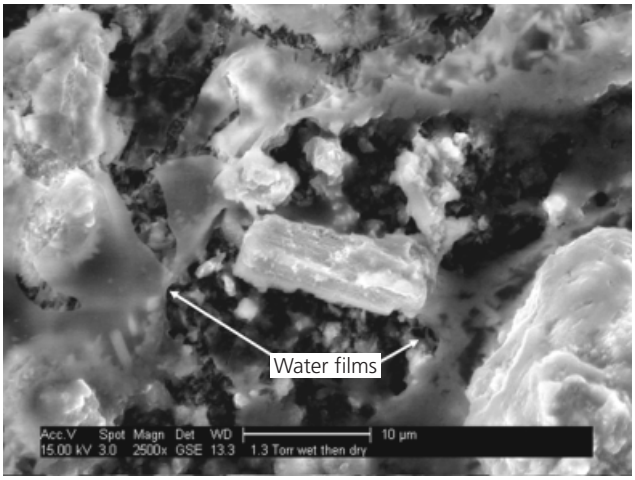

(a)

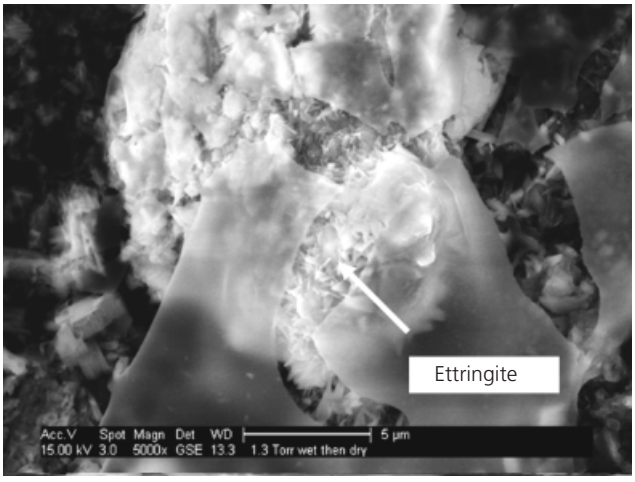

(b)

Figure 12. In situ ESEM monitoring of the pre-hydration of cubic C_3A with hemihydrate at 85% RH: (a) formation of a liquid water film within minutes after moisture exposure; (b) ettringite needles formed on the surface of a C_3A particle and water films present after 1·5 h of moisture exposure

that pre-hydration mainly occurs by way of a liquid condensed water film and less from interaction with gaseous water molecules. It also confirms the observations made before for the individual clinker phases (see Figure 5).

At lower RHs (< 60%), the liquid water films were found to be thinner compared to higher RH values. Thicker water layers enable greater ion transport, thus accelerating the chemical reactions occurring between C_3A and hemihydrate and producing more early hydration products.

The same results were obtained for the binary mixture containing cubic C_3A (images not shown here). Again, liquid water films were found in-between the particles and on the surfaces, and nano-sized ettringite crystals were identified as pre-hydration products, thus confirming a reaction between dissolved ion species.

These findings suggest that during improper storage of actual cements, capillary condensation may occur between the cement particles, initiating partial surface hydration and resulting in products identical to those formed under normal hydration conditions. Also, this process will be accelerated for cements possessing particularly small particle sizes (e.g. CEM I 52·5 type). Such cement will require more careful storage than coarser cements.

Static water vapour sorption

Complementary to the dynamic water vapour sorption, a static method was employed to examine the behaviour of the binary mixtures over longer time periods (21 d) of exposure. Figure 13 shows the sorption isotherms obtained for both mixtures over the range 23–95% RH.

The results for both static and dynamic methods were found to be in good agreement. The onset points obtained by way of the dynamic method were comparable with those from static measurements. At relative humidities below the onset points, only minor amounts of water were sorbed (less than 2 wt%). The binary mixture containing orthorhombic C_3A sorbed almost twice the amount of water compared to that containing cubic C_3A. Ettringite was found in all samples pre-hydrated above the onset point, while below those RH values no ettringite was detected. The presence of sodium ions in orthorhombic C_3A leads to a more rapid water uptake by the mixture within the first 3 d. This result implies that also in the presence of sulfate, sodium ions enhance the water uptake significantly, as was found before for the individual phases (see Figure 6).

In the SEM images of samples pre-hydrated for 21 d, again, no ettringite was observed for the samples pre-hydrated below the onset point (Figure 14). Above the threshold, however, needle-like ettringite crystals were observed. It was noticed that the shape of the ettringite crystals can vary from very thin needles produced at lower RH (75%) to long and thick crystals at 95% RH.

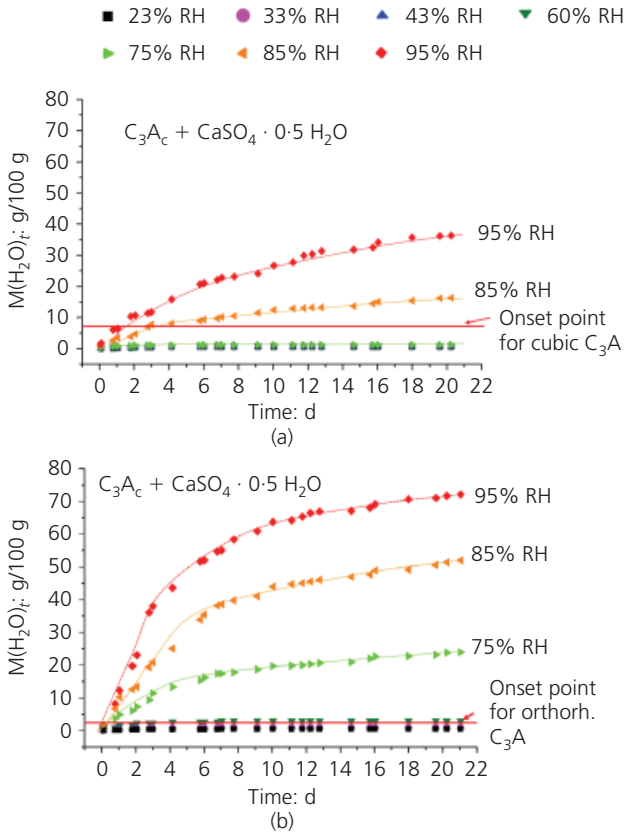

Figure 13. Water sorption isotherms for binary mixtures at 20°C and 23–95% RH as a function of time: (a) cubic C_3A + hemihydrate; (b) orthorhombic C_3A + hemihydrate

Conclusions

Dynamic and static methods of water vapour sorption were used to follow the interactions of cubic and orthorhombic C_3A polymorphs with gaseous water in the absence and in the presence of calcium sulfate hemihydrate.

It was found that both polymorphs behave differently in the presence of water vapour. The sodium ions present in orthorhombic C_3A lower the onset point to 55% RH, compared to 80% for undoped cubic C_3A. Additionally, C_3A_o sorbs a higher amount of water, which is mainly bound physically, whereas C_3A_c predominantly interacts with water chemically.

A linear relationship exists between the average particle size (d_{50} value) of a C_3A sample and the total amount of water sorbed. Smaller particles which possess higher surface areas take up more water. However, the amount of water sorbed per unit of surface area remained constant.

In the absence of sulfate, katoite was confirmed as pre-hydration product of C_3A by XRD. In the presence of calcium sulfate

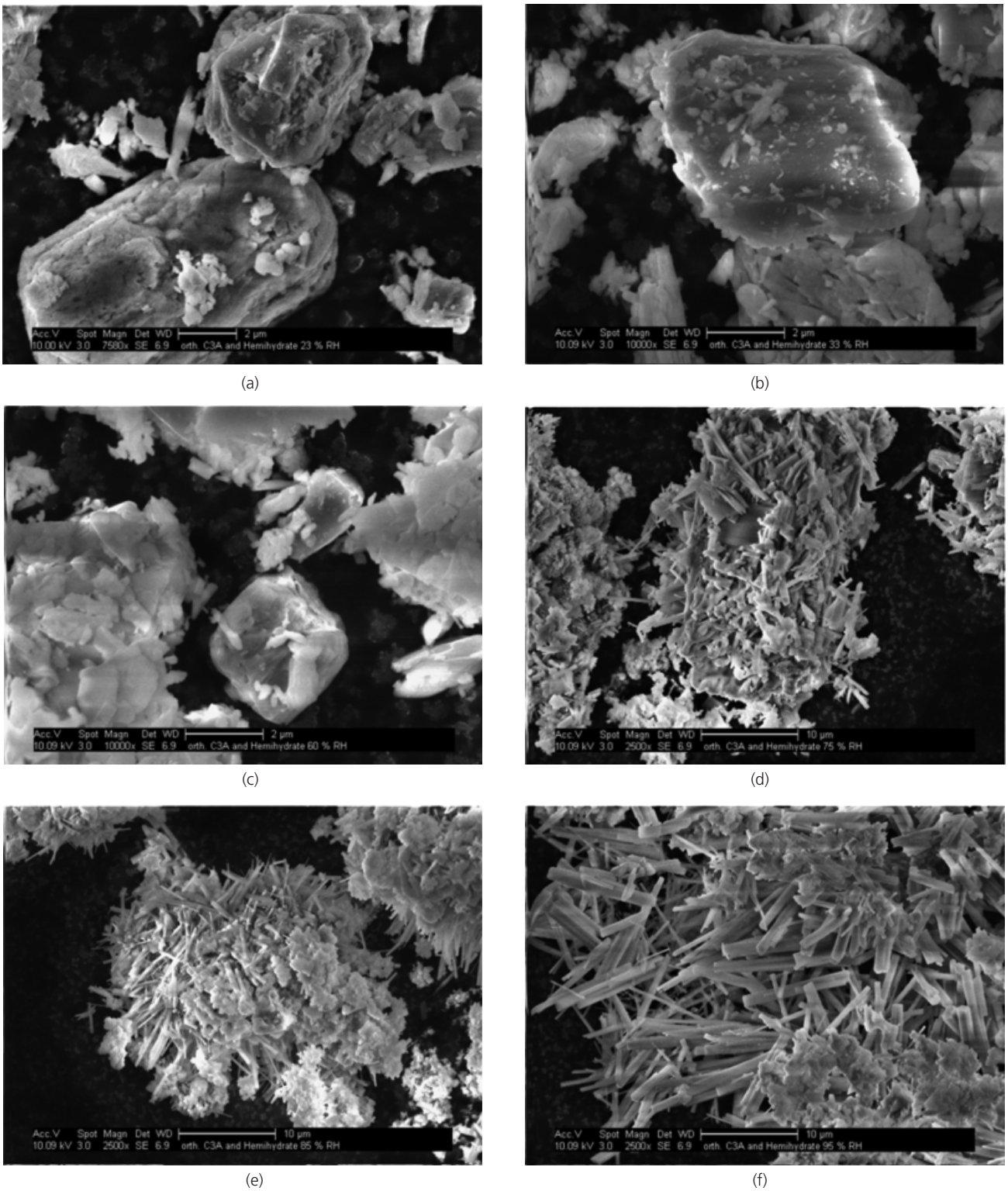

Figure 14. SEM images of orthorhombic C_3A pre-hydrated in presence of hemihydrate for 21 d at 20°C and at different relative humidities: (a) 23% RH; (b) 33% RH; (c) 60% RH; (d) 75% RH; (e) 85% RH; (f) 95% RH

hemihydrate, ettringite was found as the main pre-hydration product. ESEM imaging revealed that ettringite formation occurred by way of a condensed liquid water film. Obviously, pre-hydration not only involves surface interaction with gaseous water molecules; but also capillary condensation between C_3A particles occurs, allowing C_3A and sulfate to react according to the well-known clinker dissolution/oversaturation/precipitation scheme observed for conventional cement hydration. This finding is of fundamental importance because it signifies that during pre-hydration, similar hydrates are formed as during normal cement hydration when cement is mixed with water, although morphology might be dependent on the conditions. Ettringite crystals were shorter when RH was lower, and longer and thicker when RH increased. Below 70% RH, cubic C_3A did not react with calcium sulfate hemihydrate, while orthorhombic C_3A formed ettringite crystals already from 64% RH.

Thus, the experiments from this study suggest that when high amounts of Na-doped orthorhombic C_3A are present in a cement sample, it may undergo more pronounced pre-hydration during storage than a cement containing the same amount of cubic C_3A.

Pre-hydration occurs when the ambient RH exceeds the threshold value at which moisture uptake begins (onset point). This implies that storing cements below this critical RH value would prevent pre-hydration. Therefore, throughout the production and storage period of a cement, ideally the ambient RH should be below the onset point of the most active clinker phases. However, under actual conditions in which cement is produced, stored, distributed and used, the control of RH to the required levels practically is impossible. Careful packaging and storage are the only measures which can help to minimise the effects from pre-hydration and to extend the shelf-life stability of cement.

Acknowledgements

E. Dubina is grateful to Nanocem (core project 7) for financial support of this work. Additionally, the authors would like to thank Holger König and Maciej Zajac, HeidelbergCement, Leimen, Germany as well as Ellis Gartner, Lafarge, France for their guidance and input in many discussions.

REFERENCES

Baquerizo L, Matschei T and Scrivener K (2012) Impact of water activity on the water content of cement hydrates. *Proceedings of the Ibausil Conference*, Bauhaus-Universität, Weimar, paper number 118.

Black L, Breen C, Yarwood J *et al.* (2006) Hydration of tricalcium aluminate (C3A) in the presence and absence of gypsum – studied by Raman spectroscopy and X-ray diffraction. *Journal of Materials Chemistry* **16(13)**: 1263–1272.

Breval E (1977) Gas-phase and liquid-phase hydration of C_3A. *Cement and Concrete Research* **7(3)**: 297–304.

Breval E (1979) The effects of prehydration on the liquid hydration of $3CaO \cdot A1_2O_3$ with $CaSO_4 \cdot 2H_2O$. *Journal of the American Ceramic Society* **62(7–8)**: 395–398.

Brown PW, Libermann LO and Frohnsdorff G (1984) Kinetics of the early hydration of tricalcium aluminate in solutions containing calcium sulfate. *Journal of the American Ceramic Society* **67(12)**: 793–795.

Deng C-S, Breen C, Yarwood J *et al.* (2002) Ageing of oilfield cement at high humidity: a combined FEG-ESEM and Raman microscopic investigation. *Journal of Materials Chemistry* **12(10)**: 3105–3112.

Dubina E, Black L, Sieber R and Plank J (2010) Interaction of water vapour with anhydrous cement minerals. *Advances in Applied Ceramics* **109(5)**: 260–268.

Dubina E, Wadsö L and Plank J (2011) A sorption balance study of water vapour sorption on anhydrous cement minerals and cement constituents. *Cement and Concrete Research* **41(11)**: 1196–1204.

Glasser FP and Marinho MB (1984) Early stages of the hydration of tricalcium aluminate and its sodium-containing solid solutions. *Proceedings of the British Ceramic Society* **35**: 221–235.

Greenspan L (1977) Humidity fixed points of binary saturated aqueous solutions. *Journal of Research of the National Bureau of Standards - A, Physics and Chemistry* **81A(1)**: 89–96.

Hansen FE and Clausen HJ (1974) Cement strength and cooling by water injection during grinding. *Zement-Kalk-Gips* **27(7)**: 333–336.

JCPDS (2003) *PDF-2 Release 2003*, International Centre for Diffraction Data (ICDD), Newton Square, PA, USA.

Jensen OM (1995) Thermodynamic limitation of self-desiccation. *Cement and Concrete Research* **25(1)**: 157–164.

Jensen OM, Hansen P, Lachowski EE and Glasser FP (1999) Clinker mineral hydration at reduced relative humidities. *Cement and Concrete Research* **29(9)**: 1505–1512.

Kirchheim AP, Fernàndez-Altable V, Monteiro PJM, Dal Molin DCC and Casanova I (2009) Analysis of cubic and orthorhombic C_3A hydration in presence of gypsum and lime. *Journal of Materials Science* **44(8)**: 2038–2045.

Maltese C, Pistolesi C, Bravo A *et al.* (2007) Effect of moisture on the setting behavior of Portland cement reacting with an alkali-free accelerator. *Cement and Concrete Research* **37(6)**: 856–865.

Minard H, Garrault S, Regnaud L and Nonat A (2007) Mechanisms and parameters controlling the tricalcium aluminate reactivity in the presence of gypsum. *Cement and Concrete Research* **37(10)**: 1418–1426.

Pourchet S, Regnaud L, Perez JP and Nonat A (2009) Early C_3A hydration in the presence of different kinds of calcium sulphate. *Cement and Concrete Research* **39(11)**: 989–996.

Richartz W (1973) Effect of storage on the properties of cement. *Zement-Kalk-Gips* **26(2)**: 67–74.

Schmidt G, Bier TA, Wutz K and Maier M (2007) Characterization of the ageing behaviour of premixed dry mortars and its effect on their workability properties. *Zement-Kalk-Gips International* **60(6)**: 94–103.

Sprung S (1978) Effect of storage conditions on the properties of cements. *Zement-Kalk-Gips* **30(6)**: 305–309.

Sylla HM (1975) Effect of clinker cooling on the setting and strength of cement. *Zement-Kalk-Gips* **28(9)**: 357–362.

Theisen K and Johansen V (1975) Prehydration and strength development of Portland cement. *Journal of the American Ceramic Society* **54(9)**: 787–791.

Whittaker M, Dubina E, Al-Mutawa F *et al.* (2013) The effect of prehydration on the engineering properties of CEM I Portland cement. *Advances in Cement Research* **25(1)**: 12–20, http://dx.doi.org/10.1680/adcr.12.00030.

Winnefeld F (2008) Influence of cement ageing and addition time on the performance of superplasticizer. *Zement-Kalk-Gips International* **61(11)**: 68–77.

WHAT DO YOU THINK?

To discuss this paper, please submit up to 500 words to the editor at www.editorialmanager.com/acr by 1 April 2014. Your contribution will be forwarded to the author(s) for a reply and, if considered appropriate by the editorial panel, will be published as a discussion in a future issue of the journal.